High-Resolution Modeling of Ocean Wave and Current Fields

Okey G. Nwogu
Dept. of Naval Architecture and Marine Engineering
University of Michigan
Ann Arbor, MI 48109
phone: (734) 764-0494 fax: (734) 936-8820 email: onwogu@umich.edu

Award Number: N00014-13-1-0078

LONG-TERM GOAL

The long-term goal of this research project is to improve the Navy's capability to provide high-resolution forecasts of phase-resolved ocean wave and current fields from remotely-sensed data and our understanding of subsurface oceanic motions from their surface manifestations.

OBJECTIVES

- Develop a time-domain model for simulating highly nonlinear wave interaction with flows with an arbitrary distribution of vorticity
- Extend the model to include the effect of wave breaking and wind-wave energy transfer and validate with laboratory/field data
- Extend the model to include the effect of density stratification and nonlinear surface wave interaction with density fronts

APPROACH

This research builds on VORTWAVE, a fully-nonlinear wave model developed by Nwogu (2009) for describing the time-dependent evolution of the ocean wave and velocity fields due to:

- nonlinear wave-wave interactions
- nonlinear wave interaction with flows with an arbitrary distribution of vorticity
- wave breaking
- wind-wave growth

VORTWAVE solves the exact kinematic and dynamic free surface boundary conditions expressed as a set of evolution equations for the free surface elevation and tangential velocities at the free surface. A velocity-based boundary integral method is used to close the system of equations and relate the normal velocity of the free surface to the tangential velocities. The computational efficiency of the wave/current model is significantly improved by expanding the kernel of the boundary integral

Report Documentation Page

Form Approved
OMB No. 0704-0188

1. REPORT DATE **30 SEP 2013**	2. REPORT TYPE	3. DATES COVERED **00-00-2013 to 00-00-2013**

4. TITLE AND SUBTITLE **High-Resolution Modeling of Ocean Wave and Current Fields**	5a. CONTRACT NUMBER
	5b. GRANT NUMBER
	5c. PROGRAM ELEMENT NUMBER
6. AUTHOR(S)	5d. PROJECT NUMBER
	5e. TASK NUMBER
	5f. WORK UNIT NUMBER
7. PERFORMING ORGANIZATION NAME(S) AND ADDRESS(ES) **University of Michigan,Department of Naval Architecture and Marine Engineering,Ann Arbor,MI,48109**	8. PERFORMING ORGANIZATION REPORT NUMBER
9. SPONSORING/MONITORING AGENCY NAME(S) AND ADDRESS(ES)	10. SPONSOR/MONITOR'S ACRONYM(S)
	11. SPONSOR/MONITOR'S REPORT NUMBER(S)

12. DISTRIBUTION/AVAILABILITY STATEMENT
Approved for public release; distribution unlimited

13. SUPPLEMENTARY NOTES

14. ABSTRACT

15. SUBJECT TERMS

16. SECURITY CLASSIFICATION OF:			17. LIMITATION OF ABSTRACT	18. NUMBER OF PAGES	19a. NAME OF RESPONSIBLE PERSON
a. REPORT **unclassified**	b. ABSTRACT **unclassified**	c. THIS PAGE **unclassified**	**Same as Report (SAR)**	**6**	

Standard Form 298 (Rev. 8-98)
Prescribed by ANSI Std Z39-18

operator in terms of a wave steepness parameter and using the Fast Fourier Transform (FFT) technique to evaluate the resulting convolution integrals.

Given that VORTWAVE solves the inviscid equations of fluid motion, viscous processes such as wave breaking and wind-wave energy transfer that occur at scales much smaller than a wavelength need to be parameterized in terms of the large-scale wave motions. The effect of wave breaking is simulated in VORTWAVE by idealizing the whitecap region on the front face of spilling breaking waves as infinitely thin vortical layers that exert a vortex force on the underlying irrotational wave field. The zero-shear-stress free surface boundary condition is then used to relate the breaking-induced vorticity to the kinematics of the underlying wave field, resulting in a dissipative pressure that is proportional to the square of the normal velocity of the free surface.

WORK COMPLETED

Our initial effort focused on incorporating a Lagrangian discrete vortex model into the code to allow us to evaluate the surface signature of subsurface vortical motions in remotely sensed images of the sea surface. Two-dimensional numerical simulations were initially conducted to evaluate the ability of VORTWAVE to reproduce the results of Telste (1989) who investigated the nonlinear interaction of a pair of counter-rotating vortices with a free surface in initially calm water. The model was then utilized to investigate the interaction of a vortex pair with surface gravity waves and compared to the laboratory results of Fish (1991).

We next worked on implementing energy dissipation terms into the code to mimic the effect of wave breaking. The FFT-accelerated boundary integral wave model assumes non-overturning waves and requires an explicit specification of local regions in space and time with active breaking. Data from laboratory experiments of Chiang and Hwung (2007) were used to guide the development of a criterion for the onset of breaking. The model was then applied to the post-breaking evolution of spilling breakers to evaluate the ability of the vortex-force parameterization to describe the overall energy dissipation rate and energy dissipation process as a function of frequency.

RESULTS

Nonlinear Wave Interaction with a Pair of Counter-Rotating Vortices

We present sample results for the interaction of periodic gravity waves of wavelength λ and amplitude *A* with a pair or counter-rotating vortices in infinitely deep water. A computational domain of width 32λ was set up with a Gaussian-shaped wavemaker used to generate waves inside the domain. Damping layers were placed at both ends of the to absorb outgoing waves. Two counter-rotating vortices with circulation Γ and initial separation distrance *a* were placed at an initial depth *h*=5*a* below the still water level. Figure 1 shows a 2-D map of the stream function and vortex path for a simulation with Froude number $F_r = \Gamma / \sqrt{ga^3} = 0.5$, wavelength λ=2*a* and wave steepness *kA* = 0.2, where *k*=2π/λ. The vortices rise at constant speed $w_v = \Gamma / 2\pi a$ before being deflected near the free surface. A close-up view of the velocity field and free surface of the left vortex at $t / (a^2 / \Gamma) = 47$ is shown Figure 2. Snapshots of the wave profile at different times during the vortex motion are shown in Figure 3. The left vortex induces a strong adverse current that steepeens the waves and leads to the "scaring" of the

free surface. The wave height is also significantly reduced in the region between the two vortices. Simulations at higher Froude numbers led to instabilities due to wave breaking.

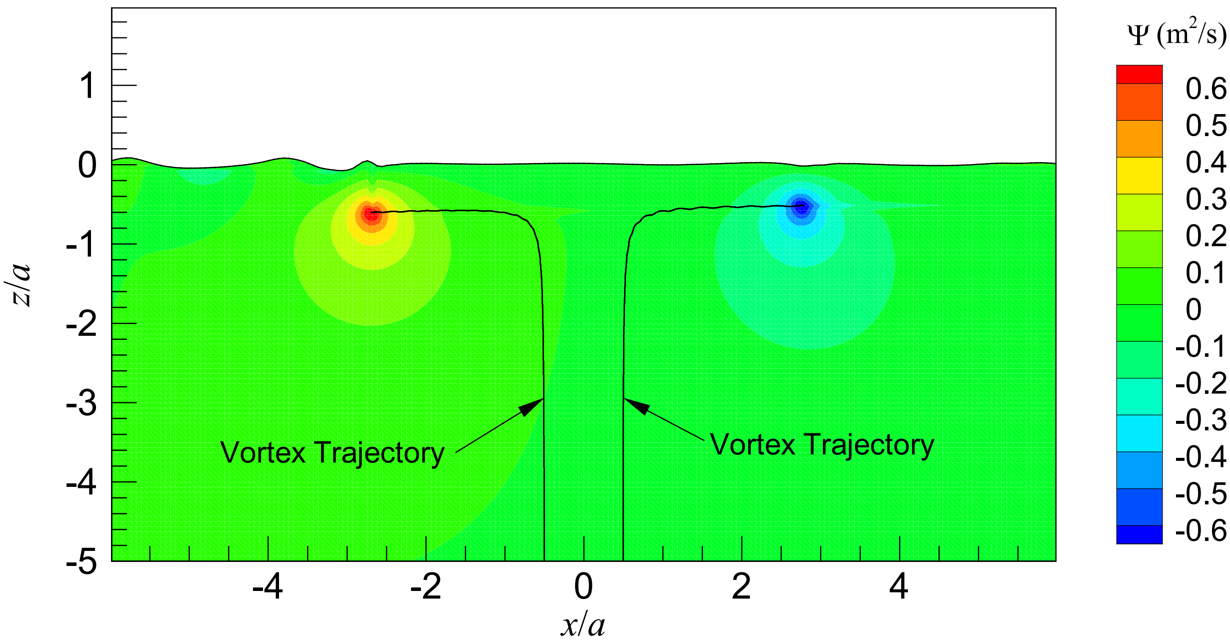

Figure 1. Vortex trajectories and stream function at $t/(a^2/\Gamma) = 47$ for nonlinear wave interaction with a pair of counter-rotating vortices ($F_r = 0.5$, $kA = 0.2$, $\lambda/a=2$).

.

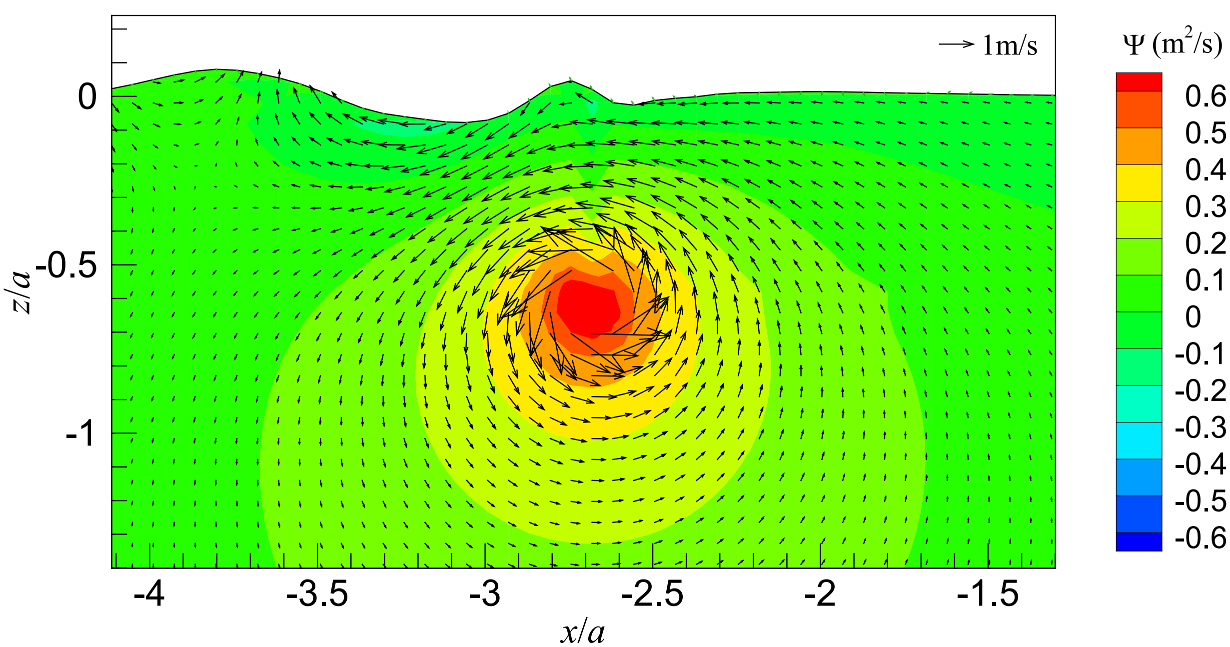

Figure 2. Close-up view of the flow field at $t/(a^2/\Gamma) = 47$ for vortex pair interacting with a surface gravity wave ($F_r = 0.5$, $kA = 0.2$, $\lambda/a=2$).

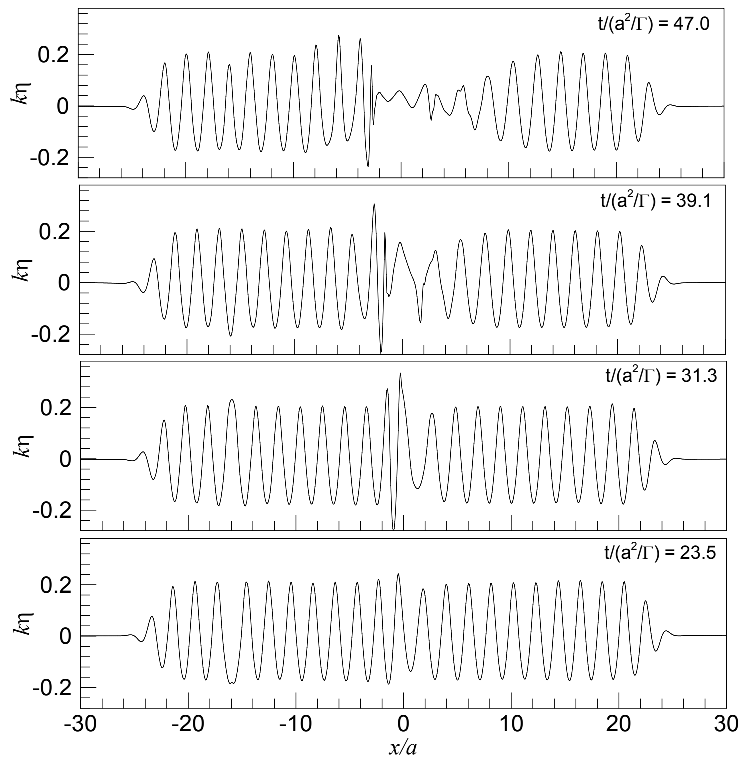

Figure 3. Modification of surface wave profile by a submerged vortex pair (F_r = 0.5, kA = 0.2, λ/a=2).

Onset of Wave Breaking

Chiang and Hwung (2007) conducted an extensive series of experiments on the evolution and breaking of modulated wave trains in the large wave flume. The incident wave train consisted of a carrier wave with amplitude A_c and frequency ω_c, and perturbations at sideband frequencies $\omega_{\pm} = \omega_c \pm \Delta\omega$ slightly detuned from the carrier wave frequency. Numerical simulations were conducted to identify a wave breaking criterion to implement in the VORTWAVE code consistent with the breaking locations observed in the laboratory experiments. Four different wave breaking criteria were evaluated including the local wave slope; the ratio of horizontal fluid velocity at crest to phase speed; the ratio of horizontal velocity gradient at crest to a characteristic frequency; and the ratio of vertical acceleration at crest to gravitational acceleration. The spatial variation of the maximum values of the different breaking criteria are plotted in Figure 4 for one of the test cases with initial wave steepness of $\varepsilon = kA_c = 0.15$. The numerical model did not become unstable at the experimental breaking location as would occur during overturning in mixed Eulerian-Lagrangian boundary integral models but further downstream when the slope of the free surface was near-vertical. The local wave slope $|\eta_x|$ at breaking is fairly close to the 30˚ angle obtained in Stokes limiting wave with a 120º corner flow at the crest. The kinematic (u_η / C) criterion, however, is much lower than the often suggested value of 1.0. Compared to the wave slope and relative crest velocity, the horizontal velocity gradient and vertical acceleration increase more rapidly just prior to breaking.

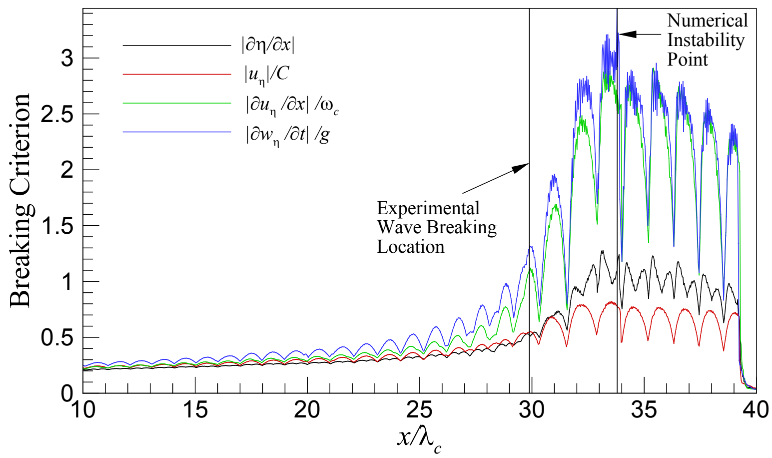

Figure 4. Spatial variation of different wave breaking criteria.

Spectral Signature of Wave Breaking

The measured water surface elevation time histories in the pre-breaking, active breaking and post-breaking regions were also analyzed to gain a better understanding of the signature of wave breaking in spectral space. Since different power laws have been proposed for the saturation range of the spectrum, the spectral densities of gauges located in the active breaking region were re-scaled by factors of ω^4 and ω^5 and are plotted in Figure 5 for three wave steepnesses (ε = 0.13, 0.15, 0.17). The different spectra appear to collapse onto a universal line in the high-frequency range. While the ω^4-scaled plot appears to show an ω^{-4} for $\omega > 3\omega_c$, the ω^5-scaled plot shows a subtle transition from ω^{-4} to ω^{-5} at $\omega \approx 5\omega_c$. The results provide further support to the hypothesis of a Kolmogorov-type cascade in breaking waves with the breaking process primarily dissipating energy transferred to the high wavenumber modes by nonlinear wave-wave interactions.

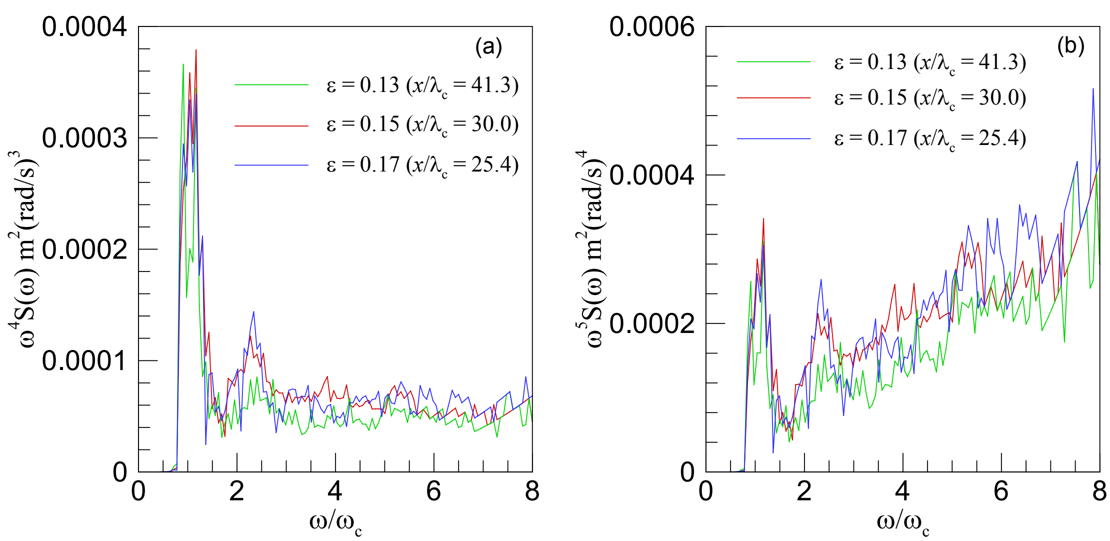

Figure 5. Frequency-scaled spectra in the active breaking region (a) scaled by ω^4 (b) scaled by ω^5.

IMPACT/APPLICATIONS

It is anticipated that this research project will lead to an improved operational tool for the real-time forecasts of ocean wave/current conditions for naval operations, techniques to identify the surface signature of submerged vortical flow structures and better parameterization of unresolved processes in phase-averaged ocean wave models.

RELATED PROJECTS

This project is closely related to the "High-Resolution Ocean Modeling" project (N00014-12-C-0566) being undertaken by David Walker at SRI. The present project is focused on developing and incorporating advanced features into the model while the SRI project is focused more on assimilating remotely sensed and other *in-situ* data into the model and evaluating the model performance with field data.

REFERENCES

Chiang, W.-S. and H.-H. Hwung. 2007. Steepness effect on modulation instability of the nonlinear wave train. *Phys. Fluids*, **19**, 014105.

Fish, S. 1991. Vortex dynamics in the presence of free surface waves. *Phys. Fluids A*, **3**, 504-506.

Nwogu, O.G., 2009. Interaction of finite-amplitude waves with vertically sheared current fields. *Journal of Fluid Mechanics*, **627**, 179-213.

Telste, J.G. 1989. Potential flow about two counter-rotating vortices approaching a free surface. *Journal of Fluid Mechanics*, **201**, 259-278.